

Титанат літію ( $\text{Li}_4\text{Ti}_5\text{O}_{12}$  або LTO) є одним з кращих варіантів заміни графіту як анодного матеріалу в літій-іонному акумуляторі (ЛІА) внаслідок утворення небажаного шару проміжної фази твердого електроліту (ПФТЕ), який споживає іон  $\text{Li}^+$ , знижує продуктивність ЛІА і може викликати некерований нагрів. Здатність LTO запобігати утворенню ПФТЕ і піддаватися нульовій деформації під час інтеркаляції робить LTO вкрай безпечним в застосуванні. Однак титанат літію зі структурою шпінелі має низьку теоретичну ємність і погану електронну провідність. Низька провідність накладає обмеження на його застосування. Золь-гель метод і об'єднання LTO з Si, що володіє високою теоретичною ємністю, є ключовим фактором в усуненні недоліків LTO. Для досягнення високої потужності, запасу міцності і маловитратних виробничих властивостей в золь-гель синтезі застосовували гідротермально-механохімічну обробку для отримання наноструктури ( $\text{Li}_4\text{Ti}_5\text{O}_{12}$ ). Потім наночастинки кремнію з масовим відсотком 5 %, 10 % і 15 % додали до електродного композиту для збільшення ємності анода титаната літію. Всі зразки були охарактеризовані з використанням рентгеноструктурного аналізу, растрової електронної мікроскопії та просвічуючої електронної мікроскопії. Активний анодний матеріал нано-LTO/Si був покритий і використаний в плоскій круглій батареї. В якості протиелектроду в зібраному плоскому круглому напівелементі використовувалася металева літієва фольга. Продуктивність батареї перевірялася за допомогою електрохімічної імпедансної спектроскопії (EIS), циклічної вольтамперометрії (ЦВ) і заряду-розряду (ЗР).

Результати рентгеноструктурного аналізу показали, що були отримані сполуки титаната літію з кристалічною структурою шпінелі ( $\text{Li}_4\text{Ti}_5\text{O}_{12}$ ) і домішками рутилу  $\text{TiO}_2$ . Результати РЕМ-мікрофотографії показали майже однорідні морфологічні структури у вигляді агломератів в більшості зразків. У той час як ПЕМ-зображення нанокремнія мало кристалічну фазу з розміром частинок менше 100 нм. Однак наявність небажаного шару  $\text{SiO}_x$  не спостерігалось чітко. Додавання наночасток Si може збільшити питому ємність вище теоретичної ємності LTO, однак, за прогнозами, утворення ізоляційного шару  $\text{SiO}_x$  є основною перешкодою, що знижує ефективність додавання наночастинок Si до з'єднання LTO. Гідротермічна обробка зразка може поліпшити характеристики нанокомпозитного анода LTO/Si. За результатами ЗР отримане з'єднання LTO/Si має розрядну здатність до 12 С.

Результати циклічної вольтамперометрії та заряду-розряду показали оптимальний масовий відсоток Si 10 %, а найкраща ємність зразка була отримана при 229,72  $\text{mAh/g}$

Ключові слова: анод  $\text{Li}_4\text{Ti}_5\text{O}_{12}$ /LTO, кремній, напівелементний акумулятор, ємність акумулятора, золь-гель, наночастинка,  $\text{TiO}_2$

UDC 621

DOI: 10.15587/1729-4061.2018.151937

# OPTIMIZING PERFORMANCE OF LITHIUM-ION BATTERY BY NANO-SILICON ADDITION MIXED IN $\text{Li}_4\text{Ti}_5\text{O}_{12}$ ANODE MADE USING MECHANOCHEMICAL-HYDROTHERMAL METHOD

B. Priyono

Doctor of Engineering in Metallurgy and Materials\*

E-mail: bambang.priyono@ui.ac.id

A. Syahrial

Professor of Engineering in Metallurgy and Materials\*

E-mail: anne@metal.ui.ac.id

A. Subhan

Research Center for Physics-LIPI PUSPIPTEK Tengerang, Banten, Indonesia, 15310

F. Faizah \*

E-mail: faizah474@yahoo.co.id

A. Gusvianty \*

\*Department of Metallurgy and Materials Engineering Universitas Indonesia Depok, Jawa Barat, Indonesia, 16424

## 1. Introduction

In recent year, lithium-ion battery technology has attracted considerable attention owing to the great potential to revolutionize the transportation industry. Rechargeable

Li-ion batteries (LIBs) play a significant role due to their high gravimetric and volumetric energy, high power density, long cycle life and low self-discharge property [1]. The spinel  $\text{Li}_4\text{Ti}_5\text{O}_{12}$  (LTO) is a highly promising anode material compared with the general graphitic carbon for use in

Li-ion batteries because attracted special attention due to its extremely small structural change during Li “intercalation/deintercalation” and the absence of solid electrolyte interface film [2], as zero-strain material, and has high thermal stability [3]. However,  $\text{Li}_4\text{Ti}_5\text{O}_{12}$  also suffers from poor electrical conductivity ( $10^{-13} \text{ S cm}^{-1}$ ) and low lithium-ion diffusion ( $10^{-9}$ – $10^{-13} \text{ cm}^2\text{-s}^{-1}$ ), which are two major issues that need to improved performance from LTO-based electrodes [4]. Spinel LTO can be synthesized by different synthesis techniques including solid-state reaction, sol-gel, high-energy ball milling, hydrothermal method, spray pyrolysis method, etc. [2]. Since the enhancement in capacity is a direct result of the composite component, silicon makes an excellent choice given its phenomenal theoretical capacity ( $4,200 \text{ mAh}\cdot\text{g}^{-1}$ ), which is 13 times higher than that of LTO [4]. Therefore, the present studies conducted are practically important and having sufficient scientific relevance.

## 2. Literature review and problem statement

The effort to increase the battery capacity continues to be done by using a variety of ways that are replacing the carbon anode with an anode containing lithium compound. LTO anodes are considered to replace carbon anodes for its few advantages that LTO has a large and stable voltage when compared to graphite (1.55 V belongs to LTO and 0 V vs. Li belongs to graphite | Li +) although LTO has a smaller capacity than the graphite anodes during the process of intercalation [5] (In numbers ranging from 170 mAh/g). Also, LTO also stable against the electrolyte can be paired with any cathode, a relatively fast charging speed [6]. No change of volume (zero strain) during the process of interstitial lithium ion, good energy efficiency, prevent decomposition of lithium thus improving battery safety, long-lasting life cycle [7] and capable of keeping pace with the steady flow of lithium ions [8], In addition to excellence, LTO material also has drawbacks, such as low  $\text{Li}^+$  ion diffusion [6] and very low theoretical capacity (175 mAh/g) [1].

Weakness in LTO material can be overcome by combining LTO with silicon nano. Battery manufacture LTO/Si aims to overcome the disadvantages of low LTO theoretical capacity (175 mAh/g). Silicon as the anode material has a large theoretical capacity reaching 4,200 mAh/g [9]. Another advantage is that silicon possessed abundant existence [10]. But in addition there are major problems owned by silicon, which is associated with a large volume expansion of silicon-owned (400 %)[4], resulting in the collapse of the electrode (pulverization) which resulted in a decrease in battery performance [11].

Based on these problems the study was performed in a blend of both superior properties owned by the two materials, namely excellent structural stability (zero strain) from LTO and high storage capacity of silicon to improve the performance of lithium-ion batteries.

In this study, will be made of Li-ion battery cells by using LTO half to add are nanoscale silicon particles with nano silicon variation of 5 wt. %, 10 wt. % and 15 wt. %. The addition of nano-sized silicon particles is done to minimize the effects of large volumes owned expansion of silicon, which is expected to improve the performance of lithium-ion batteries.

## 3. The aim and objectives of the study

This study aims to synthesize the active material for anode LIB containing the LTO which has the stable electrochemical properties and combined with the high theoretical specific capacity material in the form of Si nano and prepared into coin cell to test the performance.

To accomplish the aim, the following objectives have been set:

- preparing the active anode materials using the sol-gel method and mixing with Si nano and then fabricating a lithium battery anode-LTO/Si nano to be a Li-ion battery product half-cell;

- analyzing the influence of variation of silicon nano (5 %, 10 % and 15 %) of the performance of the battery half-cell based on the result of the EIS test, cyclic voltammetry and charge-discharge.

## 4. Materials and Methods

LTO powder was synthesized by a hydrothermal-mechanochemical method. In this study,  $\text{TiO}_2$  anatase powders were made by sol-gel and calcination process. The sol-gel process started with the mixing of the primary solution containing  $\text{Ti}(\text{C}_4\text{H}_9\text{O})_4$  and ethanol pH 3 with the secondary solution included ethanol pH 3 and distilled water. The mixing process is carried out on magnetic stirring for about 2 h until the gel formed. The obtained gel was dried in room temperature to get xerogel  $\text{TiO}_2$ . Calcination process is performed at a temperature of 300 °C for 2 hours to obtain  $\text{TiO}_2$  (anatase). Then, the hydrothermal process was done at a temperature of 120 °C for 15 h. The high energy ball mill was used to mix the result of hydrothermal with LiOH. Finally, the sintering process was then performed at 750 °C in 1 hour to form an LTO powder phase and ready to be used for the active electrode material.

The electrochemical cycling performance of LTO powder was carried out with a coin cell using a lithium metal foil as an anode. To make the anode, a slurry composition consists of active material (LTO and nano Si), acetylene black and PVDF, were measured with a weight ratio of 8:1:1. 5 grams DMAC as solvent in this mixture is also used. The measurement for each variable is presented in Table 1. Acetylene black is used as the conductive material and PVDF is used as the binder.

In this study, will be made of Li-ion battery cells with the addition of nanoscale silicon particles with nano silicon variation of 5 wt. %, 10 wt. % and 15 wt. %. Thus, the samples are denoted as LTO-n5Si, LTO-n10Si, and LTO-n15Si. Table 1 summarizes the composition of each sample.

Table 1

Mass composition and marks of each sample

| Material (wt. %) | Ratio | Mass (g) |           |           |
|------------------|-------|----------|-----------|-----------|
|                  |       | LTO-n5Si | LTO-n10Si | LTO-n15Si |
| LTO              | 80 %  | 1.0000   | 1.0000    | 1.0000    |
| Nano Si          |       | 0.0500   | 0.1000    | 0.1500    |
| Acetylene Black  | 10 %  | 0.1312   | 0.1375    | 0.1440    |
| PVDF             | 10 %  | 0.1312   | 0.1375    | 0.1440    |

The slurries were deposited on current collectors copper foil by Doctor Blade with 6 cm/minutes coating speed. The

electrode was then dried under vacuum at 80 °C for 2 h before electrochemical testing. Cell assembly was performed in a glove box filled with pure argon.

The characterization of LTO powder to know the morphology of the sample was observed by a scanning electron microscope. The particle size of the sample was measured with Image J software. Phase identification was examined by X-ray diffraction analysis (XRD) using Cu K $\alpha$  radiation. BET (Brunauer-Emmett-Teller) method was used to analyze the surface area of LTO by using Quantachrome Nova instrument.

In this work, the Li-ion battery cell was made with two electrode type cell by using LTO coin half-cell with the lithium chip as a counter electrode. The other electrode in this system would be LTO as the working electrode. The electrolyte used in this coin cells was a mixture of 1 mol LiPF<sub>6</sub> and diethyl carbonate/ethylene carbonate (1:1 in volume) solution, and Celgard polypropylene as the separator. The coin cell assembly was carried-out inside the glove box system (Vigor) under Argon ultra-high purity gas flow.

The Cyclic voltammetry (CV) of coin cell was carried out by an electrochemistry workstation (WonATech WBCS 2000) with a sweep scan rate of 0.1 mV/s and potential range between 0.1 V and 3.0 V, at a scan rate of 100  $\mu$ Vs<sup>-1</sup>. (micro-volt instead of millivolt) or equal to 0.1 mVs<sup>-1</sup>. The low potential of 0.1 V is aimed to detect the anodic/cathodic peak of Silicon and subsequent higher voltage to detect the peaks of LTO and other phases.

The galvanostatic charged-discharged on a recycler battery system (WonATech WBCS 2000) with a C-rate variation of charge and discharge (CD) testing was conducted to evaluate the cell electrochemical performance from low current (C/5) to high current (12C) discharge rate.

Electrochemical impedance spectroscopy (EIS) tests were performed to show the impedances value of electrolyte and charge transfer resistance using HIOKI RM3544 instrument with a frequency range of 0.1–20.000 Hz.

## 5. Experiment Results

The morphology of LTO powder was produced from hydrothermal mechanochemical reaction synthesis and was examined using a scanning electron microscope (SEM). Fig. 1 shows a representative SEM image of LTO powder with a magnification of 1000X and 20000X.

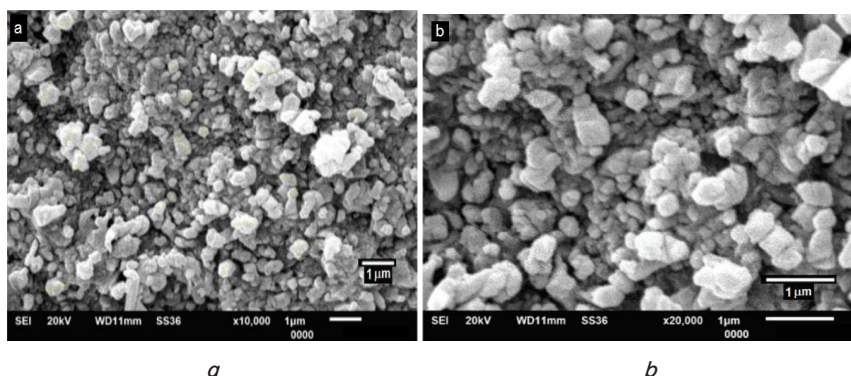


Fig. 1. SEM image of LTO powder with magnification: *a* – 10.000X; *b* – 20.000X

XRD test was performed to determine the phase of the compound that forms during the synthesis process. The

resulting data is processed using X'Pert High Score Plus software that is installed in the instrument and matches to JCPDS 00-49-0207 reference numbers for the LTO spinel phase and (JCPDS 01-076-0318) for TiO<sub>2</sub> rutile.

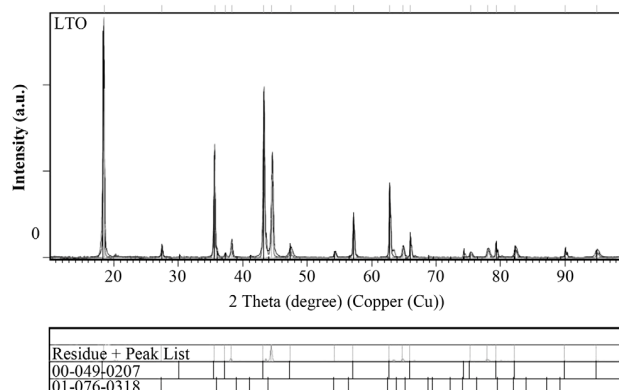


Fig. 2. XRD pattern of LTO powder after sintering for 2 h at 750 °C

Nano silicon powder in this research was observed using TEM (Transmission Electron Microscopy-Energy Dispersive X-Ray) and XRD (X-Ray Diffraction). TEM and XRD results and presence of nano-silicon particle agglomeration are shown in Fig. 3 below. In addition, X-ray Diffraction analysis was performed to identify the phase and estimate the crystallinity of nano-silicon particles. Fig 4 shows the XRD pattern that a high crystallinity of the silicon by the high-intensity peak that is formed. Besides, it also the presence of silicon oxide (Si-Ox) is positioned at 35.60° and 60.03° (JCPDS No: 00-030-1127). Four main peaks that owned Si, each position at 28.45°, 47.31°, 56.14°, 69.15° and 76.38° (JCPDS No: 00-0027-1402).

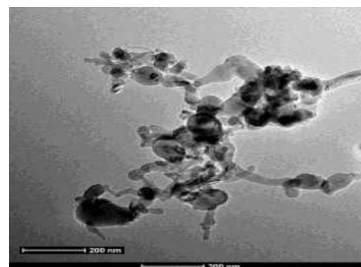


Fig. 3. Morphology of nano-silicon particles

Half-cell measurement of LTO and a lithium counter electrode using electrochemical impedance spectroscopy (EIS) can show the charge transfer resistance (*R*<sub>ct</sub>) electrode as seen in Fig. 5 as follows. Tight semicircle graph indicates better conductivity compared to that shown in wider graphs and increasing amount of silicon nano may cause lower conductivity as shown by the graph with a more widened semicircle.

The cyclic voltammetry test is conducted to examine the electrochemical performance of a lithium-ion battery.

Theoretically, LTO has a working voltage of about 1.55 V vs. cathodic lithium electrode with a theoretical capacity of

175 mAh/g [12]. The CV curve shows the initial three cycles of half-cell with a potential sweep rate of 0.1 mV/s as shown in Fig. 6. The curves show the results of cyclic Voltammetry of samples (a) LTO-n5Si, (b) LTO-n10Si and (c) LTO-n15Si. The top peak of the curve indicates the anodic peak while the curve below indicates a cathodic peak. Cathodic peak voltage shows the lithium ion intercalation process of LTO that is transformed to  $\text{Li}_7\text{Ti}_5\text{O}_{12}$  while anodic peak voltage shows de-intercalation of lithium from  $\text{Li}_7\text{Ti}_5\text{O}_{12}$  that is transformed to  $\text{Li}_4\text{Ti}_5\text{O}_{12}$ .

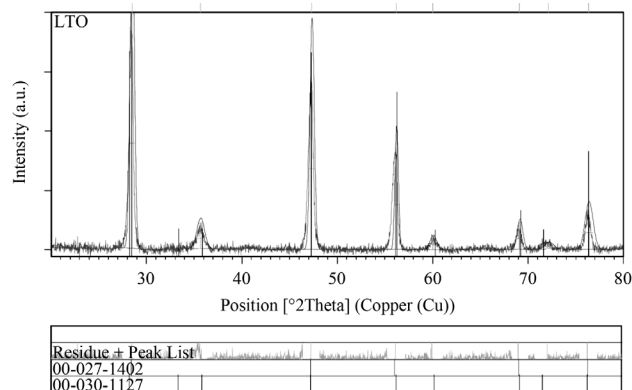


Fig. 4. XRD pattern of silicon nanopowder

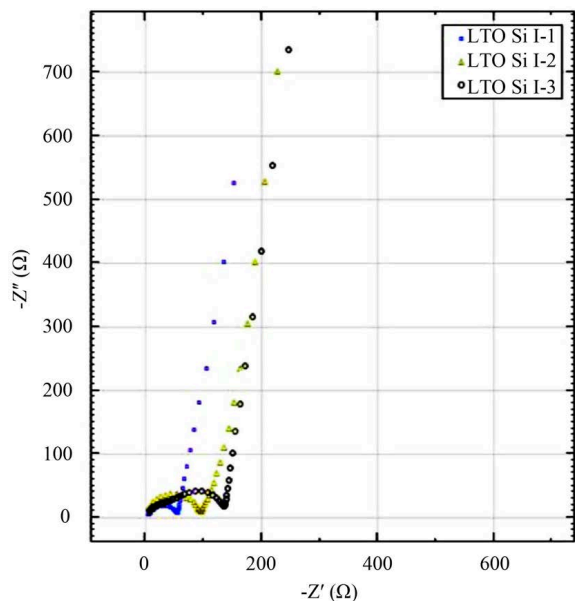


Fig. 5. Semicircle graphics of samples LTO-n5Si, LTO-n10Si and LTO-n15Si

Table 2

Charge Transfer Resistance of the sample with variation ratio weight nano-silicon particles

| Sample    | Charge Transfer Resistance (Rct) (Ω) |
|-----------|--------------------------------------|
| LTO-n5Si  | 54                                   |
| LTO-n10Si | 96                                   |
| LTO-n15Si | 136                                  |

Table 3 exhibits the battery performance from cyclic voltammetry testing. In addition, CV test results also showed the specific capacity of all samples.

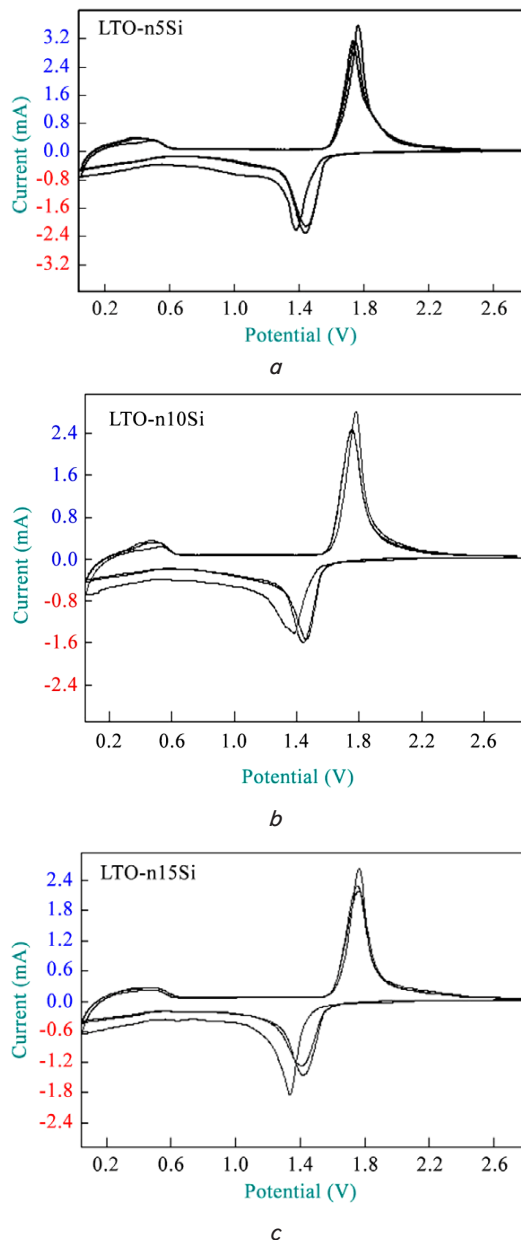


Fig. 6. Cyclic voltammetry curve of the cells: a – LTO-n5Si; b – LTO-n10Si; c – LTO-n15Si

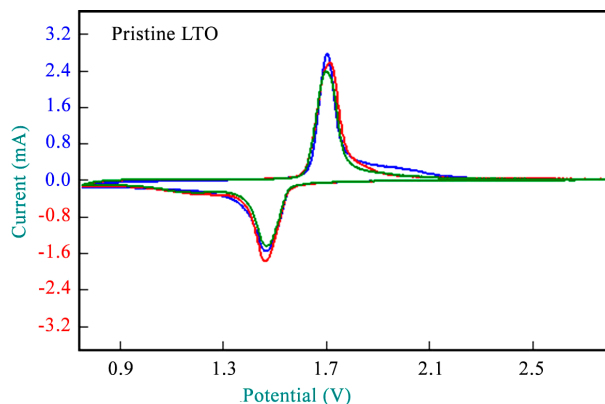


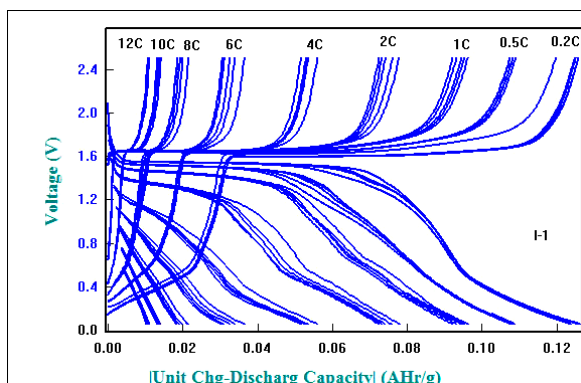
Fig. 7. Cyclic voltammetry curve of pristine LTO [13] for comparison



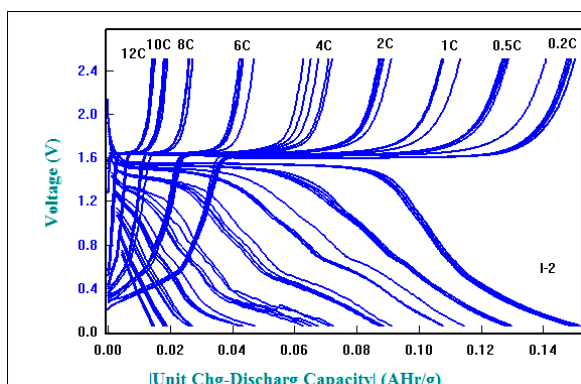
**Table 3**  
Battery performance data from cyclic voltammetry testing

| Sample    | LTO Voltage peak (V) | E (V) | Capacity (mAh/g) | ΔE (mV) |
|-----------|----------------------|-------|------------------|---------|
| LTO-n5Si  | 1.759, 1.437         | 1.59  | 187.11           | 322     |
| LTO-n10Si | 1.772, 1.445         | 1.61  | 229.72           | 327     |
| LTO-n15Si | 1.767, 1.422         | 1.60  | 207.36           | 345     |

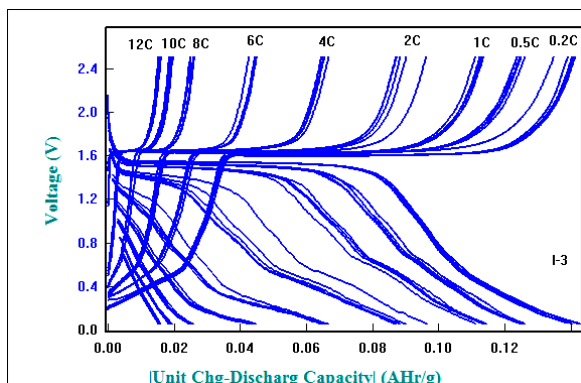
The charge and discharge (CD) tests were conducted to evaluate the cell electrochemical performance at the different current rate as shown in Fig. 5 below. Fig. 8 shows the discharge capacity of the half-cell at various nano-silicon content at C/5C to 12C with LTO powder synthesis after calcination at 750 °C for 3 h.



a



b



c

**Fig. 8.** Discharge capacity curve of half-cell with current rate C/5 to 12C of the samples: a – 5 wt %, b – 10wt %; c – 15 wt % of Si-nano

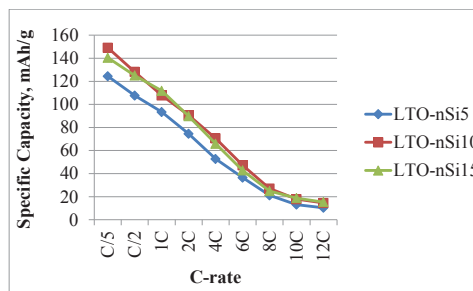


**Fig. 9.** Discharge capacity value of half-cell with current rate C/5 to 12C

Coulombic efficiency of the battery cell is shown in Fig. 10. It is interesting to note that the value of battery cell coulombic efficiency was approaching 100 %.

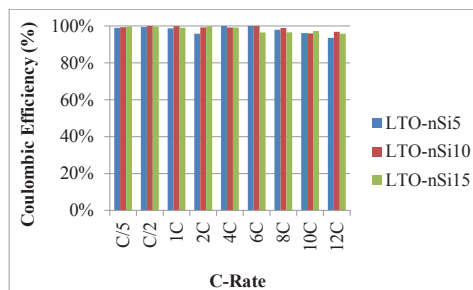


**Fig. 10.** Coulombic efficiency vs current rate of the samples (LTO-n5Si, LTO-n10Si and LTO-n15Si)

## 6. Discussion

As shown in Fig. 1, the size and morphology of LTO powder prepared using sol-gel and mechanochemical and hydrothermal processes looks having similar size and shape with a few agglomerations. The particle size of LTO can be determined by software imageJ. The average particle and agglomerate sizes of LTO were 0.52 μm and 6.43 μm, respectively.

The mechanochemical process using a ball mill followed by hydrothermal were proven to be reliable processes to prepare a solid with almost uniform shape and size.

Fig. 2 shows the peak of LTO powder after sintering for 2 h at the XRD pattern take place at 2θ: 18.29; 35.49; 43.18; 57.20; 62.78 and 66.07. It also can identify the peak of another phase as rutile TiO<sub>2</sub>. The existence of rutile TiO<sub>2</sub> is caused by the loss of Li<sup>+</sup> ions during the reaction that makes anatase TiO<sub>2</sub> are not completely reacted with Li<sup>+</sup> ion and form rutile TiO<sub>2</sub> during sintering.

Meanwhile, the nano silicon particle used in this research was observed using TEM (Transmission Electron Microscopy-Energy Dispersive X-Ray) and XRD (X-Ray Diffraction) and shows nano-silicon particle agglomeration with oxygen contamination made the SiO<sub>x</sub>. It is proved also by X-ray Diffraction analysis performed to identify the phase. The presence of silicon oxide (Si-Ox) is positioned at 35.60° and 60.03° (JCPDS No: 00-030-1127). Four main peaks that owned Si, each position at 28.45°, 47.31°, 56.14°, 69.15° and 76.38° (JCPDS No: 00-0027-1402).

Further, the general trend shows that increasing its levels of silicon nano can lead to higher resistivity values, which thus means lowering the value of conductivity. Table 2 shows

the resistivity of cell battery with a variation of silicon nano, the general trend shows that increasing its levels of silicon nano actually causes higher resistivity values, while lowering the conductivity value.  $\text{SiO}_x$  phase which has insulator properties are barriers that will reduce the conductivity of Si nano. Therefore, along with the increased levels of Si nano, the  $\text{SiO}_x$  phase is also increased. This occurrence is due to contamination of oxygen in the present silicon nano-particles which form unwanted  $\text{SiO}_x$  compound as detected in the XRD testing.

From the CV test, LTO-n5Si sample has a pair of LTO redox peaks that appeared at 1.759 V (anodic) and 1.437 V (cathodic), so the value of the working voltage is ( $E^\circ$ ) 1.59 V. The anodic nano silicon peak at 0.374 V and cathodic voltage of the nano-silicon for the three samples was the same which is close to 0 V. Then the LTO-n10Si sample has a pair of LTO redox peaks appearing at 1.772 V (anodic) and 1.445 V (cathodic). The anodic silicon nano of these samples is at 0.448 V, so the value of working voltage ( $E^\circ$ ) is 1.61 V. LTO-n15Si sample has the anodic peak at 1.767 V and cathodic peak at 1.442 V. Anodic peak of silicon nano from these samples is at 0.450 V. So the value of LTO working voltage ( $E^\circ$ ) of these samples is at 1.60 V. Anodic peak of the silicon nano comes from  $\text{Li}_x\text{Si}$  formation and the separation between anodic and cathodic peak LTO caused by the polarization resulting from the lithium ion diffusion and electrical conductivity. The average value of working voltage ( $E^\circ$ ) from all samples, i. e. 1.60 V, is not much different from LTO without silicon nanoparticles as shown in Fig. 7 [13], and the theoretical working voltage of LTO, which is about 1.55 V for lithiation process and 1.58 V for de-lithiation process [16].

Thus, the percentage of nano silicon does not have a significant influence on the formation of the working voltage of the samples. Furthermore, determination on whether the process is reversible, quasi-reversible, or irreversible can be determined from  $\Delta E_p$  equation, calculated as follows:

$$\Delta E_p = E_{p,a} - E_{p,c}, \quad (1)$$

$\Delta E_p$  value resulting from the calculation of the equation (1) obtained  $\Delta E_p$  of LTO-n5Si, LTO-n10Si and LTO-n15Si of 322 mV, 327 mV, and 345 mV, respectively. Value  $\Delta E_p$  produced in reversible reaction does not take place in three samples. This is due to the conditions for reactions to be reversible if the value of the  $\Delta E_p$  is 56–60 mV [17]. But the CV curve of all samples shows a pair of anodic and cathodic peaks, which indicate that the reaction is reversible. With both of these facts, it can be concluded that the reaction is quasi-reversible which means partially reversible.

It is predicted that the addition of Si nano on LTO will increase the capacity of lithium batteries. Table 2 shows the increasing percentage of silicon nano resulting in the decreased capacity of the battery cell. This is caused by two things, first by the agglomeration of the silicon nano. One of the challenges in using nano-sized particles is that nano-sized particles tend to agglomerate with each other. Therefore, by increasing the number of silicon nanoparticles, it resulted in the agglomeration of silicon nano increasingly preventing the lithium ions during intercalation and de-intercalation process. Secondly, it is due to the presence of an oxygen element that resulted in the formation of the passive layer of  $\text{SiO}_x$  on the electrode. Indications are observed from TEM-EDS and XRD test result. The existence of oxygen element is derived from properties of the silicon that are

unstable and from the manufacturing process of batteries that are not completely done in the glove box. So increasing the amount of silicon nano will also increase the formation of the  $\text{SiO}_x$  passive layers. It also becomes the barrier for lithium ions movements during the intercalation-deintercalation process and can cause the collapsing of specific capacity of the battery. But, the resulted capacity that is produced in this study has exceeded the theoretical capacity of LTO. The discharge capacity from LTO-n5Si samples is 187.11 mAh/g, LTO-n10Si sample is 229.72 mAh/g and LTO-n15Si is 207.36 mAh/g.

From the Charge-Discharge test, all samples show the decreasing value of specific capacity along with the current rate increase. The decrease in the specific capacity of the battery cells during the charge-discharge process occurs due to the volume expansion of the nano-silicon particles. The stress from the expansion will cause the crack and collapse of the nano-silicon that is lead to the loss of electrical contacts and capacity. However, with the addition of nano silicon variation in this study, an increase in the specific capacity of the high C-rate when compared with the results of previous studies by using the same process of LTO materials without the addition of silicon nano variations was also obtained. In one of the previous studies, specific capacity at a high C-rate can only be achieved until 10C [13]. While the results of this research, with the addition of silicon nano, specific capacity at the high C-rate can achieve up to 12C rate. From Fig. 8, 9, it is known that the addition of nano silicon increases the battery capacity at a high power rate which is required to support the need for electric vehicles battery.

The battery efficiency is also a key factor of performance. The overall value of battery cell coulombic efficiency was approaching 100 %. It is caused by the active material LTO spinel ( $\text{Li}_4\text{Ti}_5\text{O}_{12}$ ) which has zero-strain properties, so there is no change between the charge and discharge capacity of the battery [14]. Effect of the hydrothermal mechanochemical process also contributes to the efficiency achieved because the function of the hydrothermal mechanochemical process is to obtain a large surface area and maximize the mixing of  $\text{TiO}_2$  with LiOH when forming  $\text{Li}_4\text{Ti}_5\text{O}_{12}$ .

Coulombic efficiency value resulted in this study is more stable than the coulombic efficiency of LTO without hydrothermal mechanochemical processes with the same variations of silicon nano [15]. Efficiency is critical in the implementation of an application, in this case the application of battery in electric vehicles.

---

## 7. Conclusions

---

1. The active material LTO Spinel in the manufacture of battery half cells using  $\text{Li}_4\text{Ti}_5\text{O}_{12}$  anode resulting from hydrothermal mechanochemical was successfully mixed with Si nano-particle to improve the performance of the present anode material. The addition of nano-Si into synthesized LTO has been conducted by using the slurry-making method could increase specific capacity to 229.72 mAh/g at the 10 wt. % compared to the specific capacity of pure LTO of 146.82 mAh/g as prepared by the same method in previous studies. Also, the addition of silicon nano can increase the power density up to 12C.

2. Further addition of silicon nano does not have a significant effect due to the tendency of the agglomeration of

silicon nano and the formation of  $\text{SiO}_x$  passive layer. The coulombic efficiency of these half-cell batteries is almost close to 100 % which shows the capability of the active material LTO spinel to maintain the framework stability of this nano-composite LTO/Si anode material during charge and discharge process.

### Acknowledgments

The authors would like to thank “The Direktorat Riset dan Pengabdian Masyarakat Universitas Indonesia (DRPM-UI)” for the financial support to do this research under the grant of Riset PITTA/1062/FT/2018.

### References

1. Review on recent progress of nanostructured anode materials for Li-ion batteries / Goriparti S., Miele E., De Angelis F., Di Fabrizio E., Proietti Zaccaria R., Capiglia C. // *Journal of Power Sources*. 2014. Vol. 257. P. 421–443. doi: <https://doi.org/10.1016/j.jpowsour.2013.11.103>
2. The influence of the  $\text{TiO}_2$  particle size on the properties of  $\text{Li}_4\text{Ti}_5\text{O}_{12}$  anode material for lithium-ion battery / Wang D., Wu X., Zhang Y., Wang J., Yan P., Zhang C., He D. // *Ceramics International*. 2014. Vol. 40, Issue 2. P. 3799–3804. doi: <https://doi.org/10.1016/j.ceramint.2013.09.038>
3. Nitrogen-doped carbon coated  $\text{Li}_4\text{Ti}_5\text{O}_{12}$  nanocomposite: Superior anode materials for rechargeable lithium ion batteries / Li H., Shen L., Zhang X., Wang J., Nie P., Che Q., Ding B. // *Journal of Power Sources*. 2013. Vol. 221. P. 122–127. doi: <https://doi.org/10.1016/j.jpowsour.2012.08.032>
4. Chen C., Agrawal R., Wang C. High Performance  $\text{Li}_4\text{Ti}_5\text{O}_{12}$ /Si Composite Anodes for Li-Ion Batteries // *Nanomaterials*. 2015. Vol. 5, Issue 3. P. 1469–1480. doi: <https://doi.org/10.3390/nano5031469>
5.  $\text{TiO}_2$ /Si composites synthesized by sol–gel method and their improved electrode performance as Li-ion battery anodes / Usui H., Wasada K., Shimizu M., Sakaguchi H. // *Electrochimica Acta*. 2013. Vol. 111. P. 575–580. doi: <https://doi.org/10.1016/j.electacta.2013.08.015>
6. Influence of  $\text{Sc}^{3+}$  doping in B-site on electrochemical performance of  $\text{Li}_4\text{Ti}_5\text{O}_{12}$  anode materials for lithium-ion battery / Zhang Y., Zhang C., Lin Y., Xiong D.-B., Wang D., Wu X., He D. // *Journal of Power Sources*. 2014. Vol. 250. P. 50–57. doi: <https://doi.org/10.1016/j.jpowsour.2013.10.137>
7. High performance  $\text{Li}_4\text{Ti}_5\text{O}_{12}$  material as anode for lithium-ion batteries / Wang J., Zhao H., Wen Y., Xie J., Xia Q., Zhang T. et. al. // *Electrochimica Acta*. 2013. Vol. 113. P. 679–685. doi: <https://doi.org/10.1016/j.electacta.2013.09.086>
8. Film-shaped sol–gel  $\text{Li}_4\text{Ti}_5\text{O}_{12}$  electrode for lithium-ion microbatteries / Mosa J., Vélez J. F., Lorite I., Arconada N., Aparicio M. // *Journal of Power Sources*. 2012. Vol. 205. P. 491–494. doi: <https://doi.org/10.1016/j.jpowsour.2012.01.090>
9. Ozanam F., Rosso M. Silicon as anode material for Li-ion batteries // *Materials Science and Engineering: B*. 2016. Vol. 213. P. 2–11. doi: <https://doi.org/10.1016/j.mseb.2016.04.016>
10. Novel mesoporous silicon nanorod as an anode material for lithium ion batteries / Zhou Y., Jiang X., Chen L., Yue J., Xu H., Yang J., Qian Y. // *Electrochimica Acta*. 2014. Vol. 127. P. 252–258. doi: <https://doi.org/10.1016/j.electacta.2014.01.158>
11. Liang B., Liu Y., Xu Y. Silicon-based materials as high capacity anodes for next generation lithium ion batteries // *Journal of Power Sources*. 2014. Vol. 267. P. 469–490. doi: <https://doi.org/10.1016/j.jpowsour.2014.05.096>
12. Structure and Electrochemical Properties of Spinel  $\text{Li}_4\text{Ti}_5\text{O}_{12}$  Nanocomposites as Anode for Lithium-Ion Battery / Sun X., Hegde M., Zhang Y., He M., Gu L., Wang Y., Shu J. // *International Journal of Electrochemical Science*. 2014. Vol. 9. P. 1583–1596.
13. Optimizing the performance of  $\text{Li}_4\text{Ti}_5\text{O}_{12}$  anode synthesized from  $\text{TiO}_2$  xerogel and LiOH with hydrothermal-ball mill method by using acetylene black / Priyono B., Murti P. B., Syahrial A. Z., Subhan A. // *AIP Conference Proceedings*. 2017. doi: <https://doi.org/10.1063/1.4979221>
14. Synthesis and Characterization of Long Life  $\text{Li}_4\text{Ti}_5\text{O}_{12}$ /C Composite Using Amorphous  $\text{TiO}_2$  Nanoparticles / Li B., Ning F., He Y., Du H., Yang Q. H., Ma J. et. al. // *International Journal of Electrochemical Science*. 2011. Vol. 6. P. 3210–3223.
15. Effect of nano silicon content in half-cell Li-ion batteries performance with  $\text{Li}_4\text{Ti}_5\text{O}_{12}$  xerogel  $\text{TiO}_2$  solid-state anode materials / Syahrial A. Z., Sari N. T. A., Priyono B., Subhan A. // *AIP Conference Proceedings*. 2017. doi: <https://doi.org/10.1063/1.4979220>
16. Li-ion battery materials: present and future / Nitta N., Wu F., Lee J. T., Yushin G. // *Materials Today*. 2015. Vol. 18, Issue 5. P. 252–264. doi: <https://doi.org/10.1016/j.mattod.2014.10.040>
17. Wang J. *Analytical Electrochemistry*. John Wiley & Sons, Inc., 2006. doi: <https://doi.org/10.1002/0471790303>